Journal of Molecular Modeling (2019) 25: 10
https://doi.org/10.1007/s00894-018-3887-1

ORIGINAL PAPER

Theoretical investigations on structures, stability, energetic performance, sensitivity, and mechanical properties of CL-20/TNT/HMX cocrystal explosives by molecular dynamics simulation

Gui-Yun Hang [1] · Wen-Li Yu [1] · Tao Wang [1] · Jin-Tao Wang [1]

Received: 14 September 2018 / Accepted: 28 November 2018 / Published online: 3 January 2019

Abstract

In this article, the CL-20, TNT, HMX, CL-20/TNT, CL-20/HMX and different CL-20/TNT/HMX cocrystal models were established. Molecular dynamics method was selected to optimize the structures, predict the stability, sensitivity, energetic performance, and mechanical properties of cocrystal models. The binding energy, trigger bond length, trigger bond energy, cohesive energy density, detonation parameters, and mechanical properties of each crystal model were obtained. The influences of co-crystallization and molar ratios on performances of cocrystal explosives were investigated and evaluated. The results show that the CL-20/TNT/HMX cocrystal explosive with a molar ratio of 3:1:2 or 3:1:3 had larger binding energy and better stability, i.e., CL-20/TNT/HMX cocrystal explosive was more likely to be formed with these molar ratios. The cocrystal explosive had shorter maximal trigger bond length, but larger trigger bond energy and cohesive energy density than CL-20, namely, the cocrystal explosive had lower mechanical sensitivity and better safety than CL-20 and the safety of cocrystal model was effectively improved. The cocrystal model with a molar ratio of 3:1:2 had the best safety. The energetic performance of the cocrystal explosive with a molar ratio of 3:1:1, 3:1:2, or 3:1:3 was the best. These CL-20/TNT/HMX cocrystal models exhibited better and more desirable mechanical properties. In a word, the cocrystal model with molar ratio of 3:1:2 exhibited the most superior properties and was a novel and potential high-energy-density compound. This paper could provide practical helpful guidance and theoretical support to better understand co-crystallization mechanisms and design novel energetic cocrystal explosives.

Keywords Cocrystal explosives · Molecular dynamics · Energetic performance · Binding energy · Sensitivity · Mechanical properties

Introduction

For most kinds of energetic compounds (ECs), energetic performance (or energy density) and safety are always incompatible with each other, namely, ECs with high power also exhibited high mechanical sensitivity and poor safety, and it was more remarkable and severe for ECs with high energy density (HEDCs) [1, 2]. This problem has troubled researchers a lot and limited the development or application of ECs. At present, it is still an embarrassing difficulty and unavoidable challenge to solve this problem in some degree.

In recent years, co-crystallization [3, 4] has proven to be a superior and promising way of decreasing mechanical sensitivity and ameliorating safety of EMs. At the same time, co-crystallization also had splendid advantages or merits for ECs. For example, co-crystallization could strengthen thermal safety, improve mechanical properties, increase energy density, and reduce mechanical sensitivity and so on. Co-crystallization was a novel branch for ECs and it could be formed among different components through nonbond interaction forces, such as hydrogen bond, electrostatic energy, van der Waals (vdW) force, π-π stacking interaction energy, and halogen bond. Up to now, many different kinds of energetic cocrystals have been synthesized and investigated [5–11].

✉ Gui-Yun Hang
1910319052@qq.com

[1] School of Nuclear Engineering, Xi'an Research Institute of High-Tech, Shaanxi Xi'an 710025, People's Republic of China

2,4,6,8,10,12-hexanitro-2,4,6,8,10,12-hexaazaisowurtzitane (CL-20) was a typical kind of HEDCs and exhibited better energetic performance and power than other explosives. However, CL-20 has not witnessed its potential prospect and wide application in military or civil areas because it was quite sensitive to external stimulus and had high mechanical sensitivity, i.e., CL-20 had poor safety and could not meet the requirement of ammunitions and explosives.

In 2012, Bolton [12] dissolved CL-20 and octahydro-1,3,5,7-tetranitro-1,3,5,7-tetrazocine (HMX) into acetone and prepared a novel CL-20/HMX cocrystal explosive (molar ratio of 2:1) and explored its properties. The results showed that the detonation velocity of CL-20/HMX cocrystal explosive was about 100 m/s higher than that of pure HMX. However, the impact sensitivity was near to HMX. As we all know, HMX is a high-power explosive with high sensitivity, therefore, the sensitivity of CL-20/HMX cocrystal explosive is also relatively high to some extent. Later, Zongwei Yang [13] synthesized another cocrystal composed of CL-20 and 2,4,6-trinitrotoluene (TNT) with molar ratio of 1:1 and tested its performance. The results showed that the stability of CL-20/TNT cocrystal explosive was greatly enhanced with sensitivity effectively decreased. However, the energy density was not quite desirable. Consequently, if CL-20, TNT, and HMX could be cocrystallized together, the CL-20/TNT/HMX cocrystal explosive might have held the advantages of CL-20/TNT and CL-20/HMX cocrystals, namely, excellent energy density and low mechanical sensitivity. At the same time, the stability could also be improved. In cocrystal explosives, the molar ratio of different components would affect properties such as stability, mechanical properties, and especially the energy density and sensitivity. Therefore, it might be very significant to investigate the properties of cocrystal models with different molar ratios and estimate the influences of molar ratios on the performance of cocrystal explosives.

In this article, we mainly establish CL-20/TNT/HMX cocrystal models with different substituted patterns and molar ratios. Besides, the pure CL-20, TNT, HMX components, and CL-20/TNT, CL-20/HMX cocrystal models were also established. Molecular dynamics (MD) method was selected to optimize the structures and predict the stabilities, sensitivity, energy density, and mechanical properties of different cocrystal models. The effects of molar ratios on the performance of cocrystals were investigated and estimated. The results could help to clarify the co-crystallization mechanism and provide some useful guidance for energetic cocrystal designs.

Calculation models and methods

Molecular models of CL-20, TNT, and HMX

In this work, the crystal polymorph of CL-20 was chosen as ε-CL-20 because this polymorph was more stable and had better energetic performance than other polymorphs (α-, β-, γ-CL-20) [14, 15]. For HMX, we selected β-HMX owing to the fact that among the whole polymorphs of HMX (α-, γ-, δ-, β-), β-HMX had higher density and was the most stable and promising polymorph [16, 17]. The molecular structure and lattice parameters of ε-CL-20, TNT, and β-HMX are presented in Table 1, while the chemical models are illustrated in Figs. 1, 2, and 3, respectively.

Crystal models of CL-20/TNT and CL-20/HMX cocrystals

Based on the experimental results, the crystal models of CL-20/TNT and CL-20/HMX cocrystals were established. The molecular structure and lattice parameters of CL-20/TNT and CL-20/HMX cocrystal explosives are listed in Table 2. The primitive cell and supercell models of CL-20/TNT cocrystal explosive are illustrated in Fig. 4 and CL-20/HMX cocrystal models are presented in Fig. 5.

CL-20/TNT/HMX cocrystal models

In cocrystal models, the molar ratio of different components affects the properties of cocrystal explosives, such as stability, intermolecular interactions, density, mechanical properties, and especially the energetic performance and sensitivity. If the mass percent of high-power component was too much, the cocrystal explosive might have a high crystal density and superior energetic performance. However, the mechanical sensitivity would also be increased. Therefore, too much of a molar ratio of high energy density component would have a

Table 1 Molecular structure and lattice parameters of ε-CL-20, TNT, and β-HMX

	ε-CL-20[a]	TNT[b]	β-HMX[c]
Empirical formula	$C_6H_6O_{12}N_{12}$	$C_7H_5O_6N_3$	$C_4H_8O_8N_8$
Molecular mass	438	227	296
Crystal system	Monoclinic	Monoclinic	Monoclinic
Space group	P21/A	P21/A	P21/C
ρ (g/cm^3)	2.035	1.654	1.894
a (Å)	13.696	14.9113	6.540
b (Å)	12.554	6.0340	11.050
c (Å)	8.833	20.8815	8.700
α (°)	90.00	90.00	90.00
β (°)	111.18	110.365	124.30
γ (°)	90.00	90.00	90.00
V (Å^3)	1416.15	1761.37	519.39
Z	4	8	2

[a] The lattice parameters of ε-CL-20 were obtained from Ref. [18]

[b] The lattice parameters of TNT were obtained from Ref. [19]

[c] The lattice parameters of β-HMX were obtained from Ref. [16]

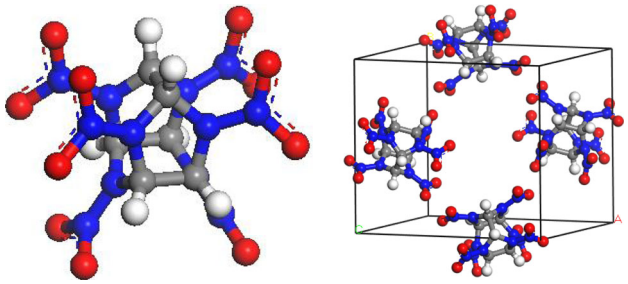

a CL -20 **b** Crystal model of ε CL-20

Fig. 1 Molecular structure of ε-CL-20

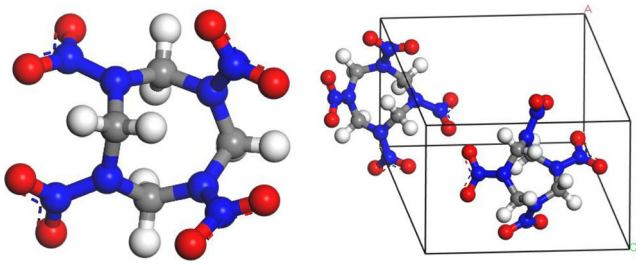

a HMX **b** Crystal model of β-HMX

Fig. 3 Molecular structure of β-HMX

positive influence on energetic performance, but a negative effect on safety of cocrystal explosives. On the contrary, if the low power component occupied too much, the cocrystal explosive might present low sensitivity. However, the energy density would be severely weakened at the same time. It was also a negative factor for cocrystal explosives. Therefore, to ensure that the cocrystal explosive has desirable energetic performance and appropriate mechanical sensitivity, the molar ratio of different components should be determined or controlled at a reasonable and proper extent.

Previous studies [13, 20–25] have illustrated that cocrystal explosives might be more likely to be formed with relatively low molar ratios. Therefore, the molar ratios of CL-20, TNT, and HMX were determined based on this principle.

At present, the substitution method is very practical and widely applied when establishing energetic cocrystal models. Therefore, in this work, the CL-20/TNT/HMX cocrystal models were established by substitution method. In other words, CL-20 molecules in supercell crystals would be substituted by TNT and HMX molecules based on the molar ratio of different components. The substitution included cleaved surfaces substitution and random substitution, namely, TNT and HMX molecules would replace the CL-20 molecules on the cleaved surfaces or randomly. To investigate the influences of co-crystallization and molar ratios on properties of cocrystal explosives and compare the performances of CL-20/TNT/HMX cocrystals with that of raw materials, we also established the crystal models of CL-20, TNT, HMX, CL-20/TNT, and CL-20/HMX cocrystals.

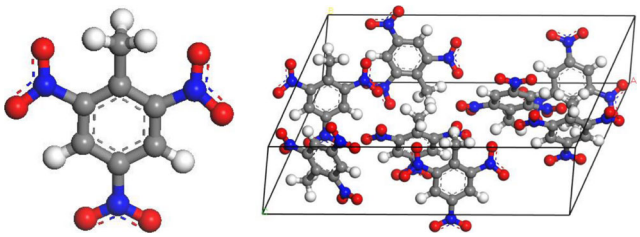

a TNT **b** Crystal model of TNT

Fig. 2 Molecular structure of TNT

The molar ratio, supercell pattern, total number of CL-20, TNT, HMX molecules, and atoms in cocrystal models are listed in Table 3.

For example, when the molar ratio of the three components (CL-20:TNT:HMX) was in 2:1:1, the CL-20/TNT/HMX cocrystal model was established as follows: Firstly, the single unit cell of ε-CL-20 was established; then it was expanded to 16 (4 × 2 × 2) supercells and 64 CL-20 molecules were included in the supercell; next, the supercell model was cleaved into (1 0 0), (0 1 0), and (0 0 1) surfaces, and shown in Fig. 6; afterwards, a vacuum layer with the thickness of 0 Å would be added into the three cleaved surfaces along the *c* crystallographic axis; finally, 16 TNT and 16 HMX molecules would substitute 32 CL-20 molecules on the three cleaved surfaces or CL-20 molecules in the initial supercell crystal model.

When the initial CL-20/TNT/HMX cocrystal model was established, the structure would be optimized with total

Table 2 Crystal structure and lattice parameters of CL-20/TNT and CL-20/HMX cocrystal explosives

	CL-20/TNT[a]	CL-20/HMX[b]
Empirical formula	$C_{13}H_{11}O_{18}N_{15}$	$C_{16}H_{20}O_{32}N_{32}$
Molecular mass	665	1172
Molar ratio	1:1	2:1
Crystal system	Orthorhombic	Monoclinic
Space group	Pbca	P21/C
ρ (g/cm^3)	1.846	2.000
a (Å)	9.7352	16.3455
b (Å)	19.9126	9.9361
c (Å)	24.6956	12.1419
α (°)	90.00	90.00
β (°)	90.00	99.233
γ (°)	90.00	90.00
V (Å^3)	4787.32	1946.42
Z	16	6

[a] The crystal parameters of CL-20/TNT cocrystal explosive were obtained from Ref. [13]

[b] The crystal parameters of CL-20/HMX cocrystal explosive were obtained from Ref. [12]

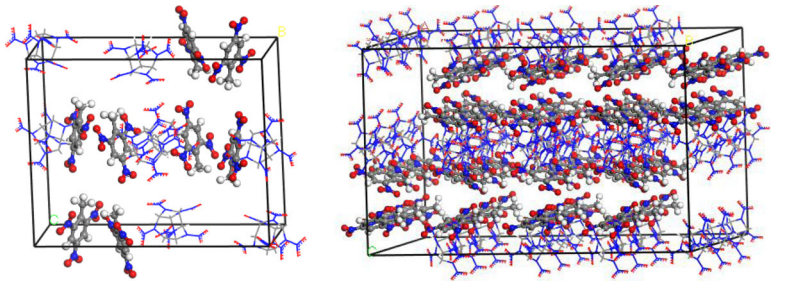

a Primitive unit cell of CL-20/TNT **b** (3×2×1) supercells of CL-20/TNT cocrystal models

Fig. 4 Primitive unit cell (**a**) and (3 × 2 × 1) supercells (**b**) of CL-20/TNT cocrystal models

energy of cocrystal model minimized. For example, when the substitution was on (0 0 1) crystal surface, the cocrystal model after optimization is presented in Fig. 7.

Calculation conditions and details

In this work, the crystal models of pure components (CL-20, TNT, and HMX) and CL-20/TNT, CL-20/HMX, and CL-20/TNT/HMX cocrystal explosives were established. The structures and energies were optimized and properties of different models were predicted through MD method. The influences of molar ratio on stability, sensitivity, energetic performance, and mechanical properties of cocrystal explosives were investigated and evaluated. To accurately predict the properties of cocrystal models, COMPASS force field [26–28] was selected because this force field was suitable for numerous materials in condensed phase. At the same time, the parameters in COMPASS force filed were validated with the correlated algorithms modified to improve the applicability and ensure its accuracy. At present, COMPASS force field was regarded as an advanced or splendid force filed and had been applied widely to determine parameters and predict the properties of materials, including energetic materials. The thermostat and barostat was set as Anderson, Parrinello, respectively. To determine the nonbond energies, such as van der Waals (vdW) and electrostatic interactions, we selected atom-based summation method for vdW and Ewald method for electrostatic. In the MD simulation, NPT ensemble was chosen and the temperature and pressure was set as 295 K, 0.0001 GPa, respectively. The temperature, pressure, and total number of atoms in crystal models would be kept constant. The step size was 1 fs and total MD simulation time was 2 ns (2×10^6 fs). At first, the crystal model would be under a MD simulation for 1 ns (1×10^6 fs) to optimize the structures, total energies, nonbond energies, and to make the system reach the equilibrium state. Then, the optimized model would be under another MD simulation for 1 ns (1×10^6 fs) to determine the parameters and energies.

Results and discussion

Choice of force field

The force field would directly affect the parameters of crystal systems and each force field might be only suitable for limited crystal models. To choose the most suitable force field and ensure the precision, we performed MD simulations with PCFF, COMPASS, Universal, and Dreiding force field. Besides, the calculated parameters were compared with experimental results.

The calculated crystal parameters and density of pure components (CL-20, TNT, HMX), CL-20/TNT and CL-20/HMX cocrystal models with NPT ensemble (295 K and 0.0001 GPa) by different force field are presented in Table 4.

As presented in Table 4, it could be concluded that the calculated results obtained by the COMPASS force field were very accurate and it was in good agreement with experimental results, thus implying that this force field was suitable for CL-20, TNT, HMX, CL-20/TNT, and CL-20/

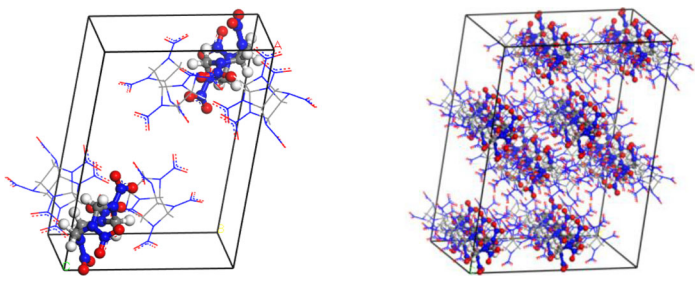

a Primitive unit cell of CL-20/HMX **b** (2×3×2) supercells of CL-20/HMX cocrystal models

Fig. 5 Primitive unit cell (**a**) and (2 × 3 × 2) supercells (**b**) of CL-20/HMX cocrystal models

Table 3 Molar ratio, supercell pattern, total number of molecules and atoms of CL-20,TNT, HMX, CL-20/TNT, CL-20/HMX, and CL-20/TNT/HMX cocrystal models

Molar ratio (CL-20:TNT:HMX)	Supercell pattern	N(total)[a]	N(CL-20)[b]	N(TNT)[c]	N(HMX)[d]	N(atoms)[e]
1:0:0[f]	3 × 3 × 2	72	72	0	0	2592
0:1:0[g]	2 × 3 × 2	96	0	96	0	2016
0:0:1[h]	4 × 3 × 3	72	0	0	72	2016
1:1:0[i]	3 × 2 × 1	96	48	48	0	2736
2:0:1[j]	2 × 3 × 2	72	48	0	24	2400
1:1:1[k]	3 × 2 × 2	48	16	16	16	1360
1:1:2	4 × 2 × 2	64	16	16	32	1808
1:1:3	5 × 2 × 2	80	16	16	48	2256
1:2:1	4 × 2 × 2	64	16	32	16	1696
1:2:2	5 × 2 × 2	80	16	32	32	2144
1:2:3	4 × 3 × 2	96	16	32	48	2592
1:3:1	5 × 2 × 2	80	16	48	16	2032
1:3:2	4 × 3 × 2	96	16	48	32	2480
1:3:3	7 × 2 × 2	112	16	48	48	2928
2:1:1	4 × 2 × 2	64	32	16	16	1936
2:1:2	5 × 2 × 2	80	32	16	32	2384
2:1:3	4 × 3 × 2	96	32	16	48	2832
2:2:1	5 × 2 × 2	80	32	32	16	2272
2:2:3	7 × 2 × 2	112	32	32	48	3168
2:3:1	4 × 3 × 2	96	32	48	16	2608
2:3:2	7 × 2 × 2	112	32	48	32	3056
2:3:3	4 × 4 × 2	128	32	48	48	3504
3:1:1	5 × 2 × 2	80	48	16	16	2512
3:1:2	4 × 3 × 2	96	48	16	32	2960
3:1:3	7 × 2 × 2	112	48	16	48	3408
3:2:1	4 × 3 × 2	96	48	32	16	2848
3:2:2	7 × 2 × 2	112	48	32	32	3296
3:2:3	4 × 4 × 2	128	48	32	48	3744
3:3:1	7 × 2 × 2	112	48	48	16	3184
3:3:2	4 × 4 × 2	128	48	48	32	3632

[a] N(total) is represented for the total number of molecules in cocrystal models

[b] N(CL-20) is the total number of CL-20 molecules included in cocrystal models

[c] N(TNT) is defined as the total number of TNT molecules

[d] N(HMX) is the total number of HMX molecules

[e] N(atoms) is the total number of atoms contained in cocrystal models

[f] Molar ratio of 1:0:0 was defined as the pure ε-CL-20

[g] Molar ratio of 0:1:0 was represented for TNT

[h] Molar ratio of 0:0:1 was defined as the pure β-HMX

[i] Molar ratio of 1:1:0 was defined as the CL-20/TNT cocrystal model

[j] Molar ratio of 2:0:1 was represented for CL-20/HMX cocrystal model

[k] Molar ratio of 1:1:1, 2:2:2, and 3:3:3 were the same

HMX cocrystals. At the same time, the data in Table 4 also indicate that the COMPASS force field was reasonable for MD simulations. Previous studies [29–33] have also pointed out that the COMPASS force field is very practical for predicting parameters and properties of large numbers of energetic materials.

Binding energy

Binding energy (E_b) was mainly defined as the intermolecular interactions between different kinds of molecules. Binding energy was an important criterion to reflect or estimate the stability of explosives. Besides, binding energy could also

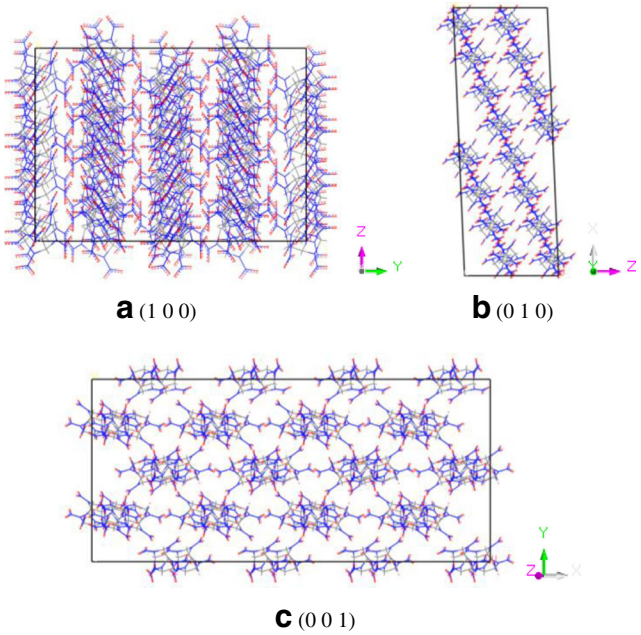

Fig. 6 Cleaved surfaces (1 0 0), (0 1 0), and (0 0 1) of (4 × 2 × 2) supercell of CL-20

be applied to evaluate the compatibility or miscibility of different components. Generally speaking, if the value of E_b was higher, it would mean that the interaction energies between different molecules were stronger and the explosive had desirable stability and favorable compatibility [29, 30, 32]. For cocrystal explosives, binding energy could also predict the formation probability. That is to say, cocrystal models with a higher value of E_b might be formed more easily or probably. In this work, the cocrystal explosive consisted of CL-20, TNT, and HMX. We were mainly concerned about the interaction energy and compatibility between CL-20 and other components, i.e., the binding energy between CL-20 and TNT, HMX molecules in cocrystal models.

Binding energy was determined by the total energy of the whole system and individual energy of each component. Binding energy was depicted as follows:

$$E_b = -E_{inter} = -\left[E_{total} - \left(E_{CL-20} + E_{TNT/HMX}\right)\right] \quad (1)$$

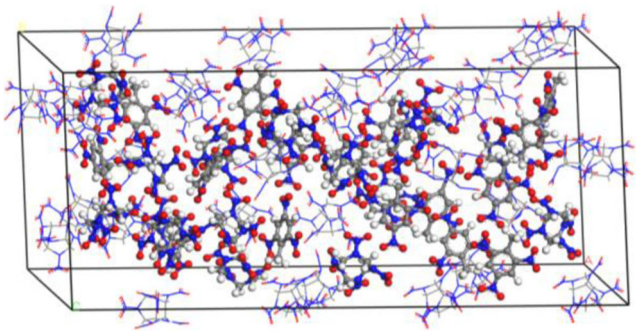

Fig. 7 CL-20/TNT/HMX cocrystal model on (0 0 1) crystal surface with molar ratio of 2:1:1

$$E_b^* = \frac{E_b \times N_0}{N_i} \quad (2)$$

where E_{inter} is defined as the interaction energy, E_{total} is defined as the total energy of cocrystal model when it was under equilibrium state, E_{CL-20} is the total energy of CL-20 molecules with all the TNT and HMX molecules moved away from the cocrystal model, $E_{TNT/HMX}$ is the total energy of TNT and HMX molecules when all the CL-20 molecules were removed, E_b^* is called the relative binding energy or corrected binding energy, N_i is the total number of molecules (including CL-20, TNT, and HMX) for *i*th cocrystal model, N_0 was the total number of molecules for a standard cocrystal model. In this work, the CL-20/TNT/HMX cocrystal model with a molar ratio of 1:1:1 was selected as the standard pattern, i.e., $N_0 = 48$.

Binding energy of CL-20/TNT/HMX cocrystal models with different substituted patterns and molar ratios is illustrated in Table 5.

From Table 5, it was concluded that the binding energy for each cocrystal model was different from each other. In other words, the binding energy would be affected or determined by substituted pattern and molar ratio of different components. In most cases, the binding energy varied as (0 1 0) > (0 0 1) > (1 0 0) > random, i.e., (0 1 0) crystal surface was more stable and the interaction energies between CL-20, TNT and HMX molecules on the (0 1 0) surface was stronger. Besides, Table 5 also illustrates that the highest binding energy of (1 0 0) and (0 1 0) crystal surfaces appeared at 3:1:2 (molar ratio), corresponding to 616.17 kJ/mol, 683.31 kJ/mol, respectively and it was 3:1:3 for (0 0 1) crystal surface (640.38 kJ/mol) and random substituted pattern (613.57 kJ/mol). Based on these data, it might be indicated that when the molar ratio was 3:1:2 or 3:1:3, the CL-20, TNT, and HMX molecules in cocrystal model would be combined tighter and the interaction force between these components was stronger. What's more, the cocrystal explosive with these molar ratios exhibited more desirable stability and might be formed more probably or likely in the same condition.

Sensitivity

Sensitivity was directly related to safety of ECs and it was commonly defined as the relative probability or possibility for ECs to be decomposed or exploded when subjected to different external stimulus. Sensitivity had a great effect on properties of ECs and it might be one of the most important performances for ECs in some sense. Up to now, many theories have been proposed to judge or predict the sensitivity of ECs [34–37]. In this work, we chose the trigger bond length, interaction energy of trigger bond, and cohesive energy density (CED) to evaluate the sensitivity of CL-20/TNT/HMX cocrystal explosives. This theory was put forward by Jijun Xiao [33, 38–42] and has been verified as an accurate and

Table 4 Calculated crystal parameters and density of CL-20, TNT, HMX, CL-20/TNT, and CL-20/HMX cocrystals[a]

	Force field	*a* (Å)	*b* (Å)	*c* (Å)	*α* (°)	*β* (°)	*γ* (°)	*ρ* (g/cm^3)
ε-CL-20	Experimental	13.6960	12.5540	8.8330	90.00	111.18	90.00	2.035
	PCFF	13.8253	12.7361	9.2529	88.90	113.69	90.11	1.932
	COMPASS	13.6889	12.7135	8.7708	90.00	112.27	90.00	2.026
	Universal	13.9767	12.8175	8.8619	89.16	108.83	91.74	1.919
	Dreiding	14.1152	12.6714	9.4656	90.02	114.78	87.25	1.877
TNT	Experimental	14.9113	6.0340	20.8815	90.00	110.365	90.00	1.654
	PCFF	14.5389	6.4748	21.7751	89.11	107.262	87.38	1.516
	COMPASS	15.0038	5.9872	21.0550	89.97	109.497	90.36	1.643
	Universal	15.5718	6.4381	22.0935	87.88	113.250	92.35	1.403
	Dreiding	15.1736	5.8455	22.5019	91.32	112.49	88.75	1.557
β-HMX	Experimental	6.5400	11.0500	8.7000	90.00	124.30	90.00	1.894
	PCFF	6.7522	11.4085	8.9823	92.38	126.19	91.82	1.721
	COMPASS	6.4938	11.0998	8.7456	90.00	124.71	90.32	1.889
	Universal	6.6838	11.1746	8.7362	89.76	123.08	88.91	1.825
	Dreiding	6.9451	11.6120	9.1372	87.11	120.34	93.25	1.616
CL-20/TNT	Experimental	9.7352	19.9126	24.6956	90.00	90.00	90.00	1.846
	PCFF	9.9468	19.5154	25.8233	92.02	90.14	91.15	1.763
	COMPASS	9.7475	19.9378	24.7269	90.00	90.05	90.00	1.839
	Universal	10.2321	19.7438	24.9686	88.71	91.38	90.03	1.752
	Dreiding	10.4118	20.4326	24.9644	91.34	87.26	91.50	1.664
CL-20/HMX	Experimental	16.3455	9.9361	12.1419	90.00	99.233	90.00	2.000
	PCFF	16.8035	10.1132	12.4241	91.07	99.275	92.35	1.868
	COMPASS	16.3510	9.9394	12.1460	90.04	99.181	90.02	1.998
	Universal	16.5494	10.0600	12.2933	89.35	98.766	91.05	1.927
	Dreiding	17.1156	10.4042	12.7139	88.26	101.356	88.77	1.742

[a] The crystal parameters of ε-CL-20, TNT, β-HMX, CL-20/TNT, and CL-20/HMX cocrystals were obtained from Ref. [12, 13, 16, 18, 19], respectively

practical theory. Up to now, this theory has been applied in ECs fields to predict the sensitivity of some explosives consisting of single component or multiple components.

Trigger bond length

The trigger bond of ECs was generally defined as the chemical bond that was the weakest or had the least bond energy. Compared with other chemical bonds, the trigger bond was more active and would be ruptured or broken more easily under external stimulus. For CL-20/TNT/HMX cocrystal explosives, it consisted of three components, namely, CL-20, TNT, and HMX. Among them, CL-20 was the most active component and exhibited the highest mechanical sensitivity. Therefore, CL-20 molecules would be decomposed or exploded more easily than TNT and HMX molecules under external stimulus, which would result in the next chemical reaction of cocrystal explosives. For CL-20, the N-N bond in nitro groups (N-NO_2 groups) had the least bond energy and was the weakest chemical bond. In other words, the N-NO_2 bond was the trigger bond for CL-20 [43, 44]. Consequently, the N-NO_2 bond in CL-20 molecules was chosen as the trigger bond to predict the sensitivity of CL-20/TNT/HMX cocrystal explosives.

The trigger bond length of CL-20/TNT/HMX cocrystal explosive with a molar ratio of 2:3:1 on (0 1 0) crystal surface is shown in Fig. 8. The probable trigger bond length (L_{prob}), average trigger bond length (L_{ave}), and maximum trigger bond length (L_{max}) of pure CL-20, CL-20/TNT, CL-20/HMX, and different CL-20/TNT/HMX cocrystal explosives were presented in Table 6.

It can be concluded from Fig. 8 that the trigger bond length distribution was nearly the Gauss's distribution and most of the trigger bond distributed between 1.350~1.450 Å.

Table 6 illustrates that the values of L_{prob} and L_{ave} were nearly the same for CL-20, CL-20/TNT, CL-20/HMX, and CL-20/TNT/HMX cocrystal explosives and both of them did not vary obviously, which might indicate that cocrystallization had no influence or little influence on probable trigger bond length (L_{prob}) or average trigger bond length (L_{ave}). However, the value of maximum trigger bond length (L_{max}) varied obviously for each cocrystal model. For CL-20, CL-20/TNT, and CL-20/HMX cocrystal explosives, the value of L_{max} was 1.642, 1.545, and 1.618 Å, respectfully. The

Table 5 Binding energy of different CL-20/TNT/HMX cocrystal explosives (kJ/mol)

Molar ratio (CL-20:TNT:HMX)	(1 0 0)	(0 1 0)	(0 0 1)	Random
1:1:1	503.68	547.69	541.66	477.38
1:1:2	494.25	526.73	530.03	453.61
1:1:3	466.34	515.45	500.63	447.06
1:2:1	539.27	570.38	562.71	490.40
1:2:2	535.05	564.59	543.78	481.26
1:2:3	496.56	530.36	507.34	470.70
1:3:1	529.51	554.32	543.62	511.01
1:3:2	521.17	540.44	529.60	499.52
1:3:3	490.38	523.73	505.47	487.18
2:1:1	591.25	615.84	599.70	577.29
2:1:2	583.37	603.35	572.36	573.03
2:1:3	554.30	584.48	577.61	558.07
2:2:1	577.21	594.37	581.30	560.28
2:2:3	563.16	577.61	574.26	553.58
2:3:1	526.28	543.64	530.73	520.69
2:3:2	522.35	536.91	529.04	511.48
2:3:3	490.27	516.70	499.35	466.28
3:1:1	607.21	640.79	618.55	591.60
3:1:2	616.17	683.31	635.72	595.43
3:1:3	595.74	656.56	640.38	613.57
3:2:1	585.49	620.04	606.38	577.66
3:2:2	588.73	605.78	601.40	565.37
3:2:3	570.34	591.19	577.70	552.63
3:3:1	553.06	573.64	558.92	546.71
3:3:2	526.74	552.10	549.39	531.77

maximum trigger bond length of CL-20/TNT cocrystal explosive was decreased by 5.91% than CL-20 and it was 1.46% for CL-20/HMX cocrystal explosive. Although the CL-20 molecules that had larger trigger bond length than L_{max} only occupied a small portion, these molecules were particularly active and sensitive to external stimulus, and it might be more likely for the trigger bond to be broken to make the explosive decomposed or exploded. Therefore, CL-20 had higher mechanical sensitivity than CL-20/TNT and CL-20/HMX cocrystal explosives. The L_{max} for CL-20/TNT/HMX cocrystal explosives were between that of pure CL-20 and CL-20/TNT cocrystal explosive and the cocrystal model with a molar ratio of 3:1:2 had the least value of L_{max} (1.592 Å). Generally speaking, if the value of L_{max} was larger, it would mean that the chemical bond was more active and had weaker bond strength. Consequently, the trigger bond in the CL-20/TNT/HMX cocrystal model was stabilized with bond strength enhanced. In other words, the safety of CL-20/TNT/HMX cocrystal explosive was improved or increased.

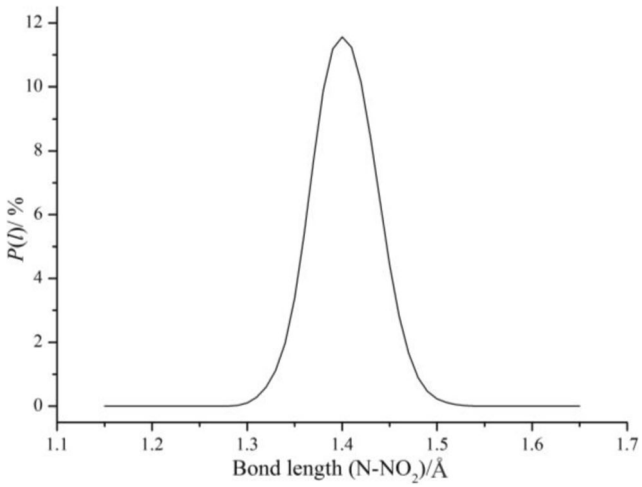

Fig. 8 Trigger bond length distribution of CL-20/TNT/HMX cocrystal explosive

Interaction energy of trigger bond

Interaction energy of trigger bond could directly reflect the bond strength. If the value of trigger bond energy was higher, it would indicate that the bond strength was stronger and the sensitivity of ECs was lower.

Interaction energy of the trigger bond was illustrated as:

$$E_{N-N} = \frac{E_T - E_F}{n} \quad (3)$$

where E_T is the total energy of the cocrystal explosive when it is under equilibrium state, E_F is the total energy of cocrystal model when all the N atoms in CL-20 molecules is constrained purposely, n is the total number of N-N bond in CL-20 molecules.

The trigger bond energy of CL-20/TNT/HMX cocrystal explosives with different molar ratios and substituted patterns are listed in Table 7.

As illustrated in Table 7, it can be concluded that CL-20/TNT, CL-20/HMX, and CL-20/TNT/HMX cocrystal explosives had higher values of trigger bond strength than raw CL-20. For example, the trigger bond energy of CL-20, CL-20/TNT, and CL-20/HMX cocrystal explosive was 138.6, 156.7, and 145.6 kJ/mol, respectively. Compared to pure CL-20, the trigger bond energy of CL-20/TNT cocrystal explosive was increased by 13.06%. For CL-20/HMX cocrystal explosive, the trigger bond energy was increased by 5.05% compared to that of CL-20. The increase of trigger bond energy illustrated that the stability and strength of trigger bond was effectively improved or enhanced, which further meant that CL-20/TNT, CL-20/HMX and CL-20/TNT/HMX cocrystal explosives had lower sensitivity and better safety than CL-20.. At the same time, the trigger bond energy also implied that co-crystallization was a superior and effective means to decrease sensitivity of ECs. Table 7 also illustrates that for the different substituted patterns, trigger bond energy ranged as (0 1 0) > (1

Table 6 Trigger bond length distribution of different CL-20/TNT/HMX cocrystal explosives (Å)

Bond length	1:0:0	1:1:0	2:0:1	1:1:1	1:1:2	1:1:3	1:2:1	1:2:2	1:2:3	1:3:1
L_{prob}	1.399	1.394	1.396	1.396	1.397	1.396	1.396	1.396	1.397	1.396
L_{ave}	1.398	1.394	1.397	1.396	1.396	1.395	1.396	1.397	1.396	1.395
L_{max}	1.642	1.545	1.618	1.608	1.606	1.607	1.605	1.611	1.608	1.601
Bond length	1:3:2	1:3:3	2:1:1	2:1:2	2:1:3	2:2:1	2:2:3	2:3:1	2:3:2	2:3:3
L_{prob}	1.396	1.397	1.398	1.396	1.396	1.396	1.396	1.397	1.396	1.397
L_{ave}	1.396	1.398	1.398	1.396	1.397	1.395	1.397	1.397	1.396	1.396
L_{max}	1.610	1.617	1.612	1.610	1.610	1.619	1.602	1.602	1.601	1.601
Bond length	3:1:1	3:1:2	3:1:3	3:2:1	3:2:2	3:2:3	3:3:1	3:3:2		
L_{prob}	1.397	1.395	1.398	1.398	1.397	1.396	1.396	1.396		
L_{ave}	1.397	1.396	1.398	1.398	1.396	1.397	1.396	1.397		
L_{max}	1.604	1.592	1.609	1.607	1.609	1.603	1.604	1.601		

0 0) > random > (0 0 1), thus indicates that (0 1 0) crystal surface was more insensitive and had the best safety. What's more, Table 7 also implies that the molar ratios of CL-20, TNT, and HMX would affect the trigger bond strength. Among the whole CL-20/TNT/HMX cocrystal explosives, the trigger bond energy for cocrystal model with molar ratio of 3:1:2 was the highest, which indicates that this cocrystal model was more insensitive and had the lowest mechanical sensitivity and the best safety.

Cohesive energy density

Cohesive energy density (CED) belonged to the nonbond energy. It was composed of vdW and electrostatic energy. CED could be defined as the total energy that is needed to separate all the explosive molecules from each other. The CED, vdW, and electrostatic energies of different CL-20/TNT/HMX cocrystal explosives are shown in Table 8.

As shown in Table 8, it was concluded that CL-20 (molar ratio of 1:0:0) had the least value of CED, vdW, and electrostatic energies, corresponding to 0.638, 0.176, and 0.462 kJ/cm^3, respectively. CL-20/TNT cocrystal explosive (molar ratio of 1:1:0) exhibited the largest value of CED (0.855 kJ/cm^3), vdW (0.243 kJ/cm^3), and electrostatic energy (0.612 kJ/cm^3). These energies of CL-20/TNT cocrystal explosive were increased by 34.01, 38.07, and 32.47% when compared to that of pure CL-20, thus illustrating that the sensitivity of CL-20/TNT cocrystal explosive was greatly decreased. Among the different CL-20/TNT/HMX cocrystal models, the value of CED, vdW, and electrostatic energy was higher than pure CL-20 and CL-20/HMX cocrystal explosive, but lower than CL-20/TNT cocrystal explosive. Table 8 also shows that when the molar ratio was 3:1:2, the nonbond energies, including CED, vdW, and electrostatic energies, were the largest, corresponding to 0.797, 0.233, and 0.564 kJ/cm^3. The CED was increased by 24.92% compared pure CL-20, and it was 32.39% for vdW energy and 22.08%

Table 7 Interaction energy of trigger bond of different CL-20/TNT/HMX cocrystal explosives (kJ/mol)

Substituted pattern	1:0:0	1:1:0	2:0:1	1:1:1	1:1:2	1:1:3	1:2:1	1:2:2	1:2:3	1:3:1
(1 0 0)	138.6	156.7	145.6	148.4	146.6	146.2	150.2	148.6	147.9	152.9
(0 1 0)	144.9	169.8	153.4	157.6	156.4	159.3	159.4	157.1	155.3	160.7
(0 0 1)	132.1	146.2	136.3	144.5	140.8	139.9	145.3	144.2	142.0	144.2
Random	134.5	153.3	140.8	146.3	143.1	143.0	148.5	146.4	146.1	150.9
Substituted pattern	1:3:2	1:3:3	2:1:1	2:1:2	2:1:3	2:2:1	2:2:3	2:3:1	2:3:2	2:3:3
(1 0 0)	151.1	149.8	147.9	149.9	149.9	148.4	147.5	146.9	149.1	145.9
(0 1 0)	158.4	154.6	152.7	155.7	156.1	153.2	154.3	154.5	154.3	153.9
(0 0 1)	142.7	141.2	141.3	142.0	143.1	142.5	141.4	143.8	142.0	143.6
Random	148.3	147.3	147.7	148.4	147.4	148.1	148.2	145.0	148.7	144.9
Substituted pattern	3:1:1	3:1:2	3:1:3	3:2:1	3:2:2	3:2:3	3:3:1	3:3:2		
(1 0 0)	146.9	154.9	154.0	152.3	150.5	148.6	151.6	148.0		
(0 1 0)	154.3	163.6	160.8	159.9	157.7	152.4	159.5	157.1		
(0 0 1)	143.9	145.0	143.7	143.5	145.6	145.2	145.5	144.3		
Random	144.7	151.2	150.9	150.7	149.8	147.7	150.6	145.6		

Table 8 CED, vdW, and electrostatic energies of CL-20/TNT/HMX cocrystal explosives (kJ/cm^3)[a]

Parameter	1:0:0	1:1:0	2:0:1	1:1:1	1:1:2	1:1:3	1:2:1	1:2:2	1:2:3	1:3:1
CED	0.638	0.855	0.687	0.710	0.707	0.705	0.724	0.715	0.712	0.783
vdW	0.176	0.243	0.193	0.203	0.202	0.201	0.218	0.211	0.210	0.242
Electrostatic	0.462	0.612	0.494	0.507	0.505	0.504	0.506	0.504	0.502	0.541
Parameter	1:3:2	1:3:3	2:1:1	2:1:2	2:1:3	2:2:1	2:2:3	2:3:1	2:3:2	2:3:3
CED	0.778	0.769	0.708	0.727	0.735	0.719	0.750	0.753	0.757	0.753
vdW	0.241	0.236	0.205	0.218	0.219	0.209	0.228	0.228	0.229	0.227
Electrostatic	0.537	0.533	0.503	0.509	0.516	0.510	0.522	0.525	0.528	0.526
Parameter	3:1:1	3:1:2	3:1:3	3:2:1	3:2:2	3:2:3	3:3:1	3:3:2		
CED	0.760	0.797	0.791	0.780	0.775	0.767	0.781	0.773		
vdW	0.231	0.233	0.230	0.225	0.224	0.219	0.223	0.219		
Electrostatic	0.529	0.564	0.561	0.555	0.551	0.548	0.558	0.554		

[a] CED = vdW + Electrostatic

for electrostatic energy. These data meant that the CL-20/TNT/HMX cocrystal explosive model with molar ratio of 3:1:2 had the lowest mechanical sensitivity, but the best safety.

Detonation performance

The power and energetic performance of ECs could be reflected by correlated detonation parameters, such as detonation velocity (D), detonation pressure (P), and detonation heat (Q). In this work, the nitrogen equivalent coefficient (NEC) method was chosen to calculate the detonation parameters and predict the energy density of cocrystal explosives and raw components. The NEC method was first put forward in 1964 and later revised by Housheng Zhang in 1978 [45]. The NEC method took some factors that might affect or determine the detonation parameters into consideration, such as molecular structure, detonation products, the chemical bond, or chemical groups existing in explosives. Therefore, the NEC method was a very practical and precise method for numerous different kinds of explosives.

For ECs that only contained C-H-O-N element ($C_aH_bO_cN_d$), the oxygen balance (OB) was depicted as follows:

$$OB = \frac{[c-(2a+b/2)]}{M_r} \times 16 \times 100\% \quad (4)$$

where a, b, c, and d are the total number of carbon, hydrogen, oxygen, and nitrogen atoms existing in explosive molecules, and M_r is the molar mass of explosive with the unit of g/mol.

The value of OB for mixed explosives could be obtained as:

$$OB = \sum w_i OB_i \quad (5)$$

where w_i is the mass percent of ith component in mixed explosive and OB_i is the oxygen balance of ith component.

According to NEC method, detonation parameters (D and P) could be calculated as that:

$$\begin{cases} D = (690 + 1160\rho_0)\sum N_{\mathrm{ch}} \\ P = 1.106(\rho_0 \sum N_{\mathrm{ch}})^2 - 0.84 \\ \sum N_{\mathrm{ch}} = \dfrac{100}{M_r}\left(p_i N_{pi} + \sum B_K N_{BK} + \sum G_j N_{Gj}\right) \end{cases} \quad (6)$$

where $\sum N_{\mathrm{ch}}$ is the total nitrogen equivalent coefficient, p_i, N_{pi}, B_K, N_{BK}, G_j, N_{Gj} are the correlated parameters determined by explosive molecules, detonation products, chemical bonds, and chemical groups. All of the parameters in Eq. (6) are interpreted in Refs. [46, 47]. To better understand the NEC method, we could consult Refs. [46, 47] for more information and further help.

The detonation products and nitrogen equivalent parameter of raw components, such as CL-20 ($C_6H_6O_{12}N_{12}$), TNT ($C_7H_5O_6N_3$), and HMX ($C_4H_8O_8N_8$) were determined based on the H_2O-CO-CO_2 principle, i.e., the detonation equations of these three explosives were illustrated as:

$$\begin{cases} C_6H_6O_{12}N_{12} \rightarrow 3H_2O + 3CO + 3CO_2 + 6N_2 \\ C_7H_5O_6N_3 \rightarrow 2.5H_2O + 3.5CO + 3.5C + 1.5N_2 \\ C_4H_8O_8N_8 \rightarrow 4H_2O + 4CO + 4N_2 \end{cases} \quad (7)$$

Detonation heat (Q) is depicted as follows [48, 49]:

$$Q = \sum \omega_i Q_i \quad (8)$$

where Q is the detonation heat of mixed explosive and ω_i and Q_i are the mass percent and detonation heat of ith component, respectively.

The detonation parameters of raw components (CL-20, TNT, HMX), CL-20/TNT, CL-20/HMX, and CL-20/TNT/HMX cocrystal explosives are presented in Table 9.

From Table 9 it can be concluded that the density (ρ) and detonation parameters (D, P, Q) of raw CL-20 was 2.035 g/cm^3, 9.50 km/s, 46.60 GPa, 6230 kJ/kg, respectively. The high value of density and detonation parameters mean that CL-20

Table 9 Detonation parameters of raw components, CL-20/TNT, CL-20/HMX, and CL-20/TNT/HMX cocrystal explosives

Molar ratio (CL-20:TNT:HMX)	Mass percent (%)			ρ (g/cm^3)	*OB* (%)	*D* (km/s)	*P* (GPa)	*Q* (kJ/kg)
	w(CL-20)	*w*(TNT)	*w*(HMX)					
1:0:0	100	0	0	2.035	− 10.96	9.50	46.60	6230
0:1:0	0	100	0	1.654	− 74.00	7.08	21.45	4570
0:0:1	0	0	100	1.894	− 21.62	9.05	39.45	6190
1:1:0	65.86	34.14	0	1.909	− 32.48	8.87	36.73	5663
2:0:1	74.74	0	25.26	1.997	− 13.65	9.39	43.08	6220
1:1:1	45.58	23.62	30.80	1.889	− 29.13	8.90	36.84	5826
1:1:2	34.84	18.06	47.10	1.890	− 27.37	8.96	37.36	5911
1:1:3	28.20	14.62	57.18	1.891	− 26.27	9.00	37.69	5964
1:2:1	36.87	38.22	24.91	1.839	− 37.71	8.52	33.23	5586
1:2:2	29.51	30.59	39.90	1.849	− 34.50	8.65	34.34	5706
1:2:3	24.61	25.50	49.89	1.857	− 32.36	8.73	35.09	5787
1:3:1	30.95	48.13	20.92	1.806	− 43.54	8.27	30.98	5423
1:3:2	25.60	39.80	34.60	1.821	− 39.74	8.42	32.27	5555
1:3:3	21.82	33.93	44.25	1.832	− 37.07	8.53	33.21	5649
2:1:1	62.61	16.23	21.16	1.932	− 23.45	9.19	39.69	5952
2:1:2	51.68	13.39	34.93	1.925	− 23.13	9.18	39.59	5994
2:1:3	44.00	11.40	44.60	1.921	− 22.90	9.18	39.52	6023
2:2:1	53.87	27.93	18.20	1.888	− 30.51	8.86	36.43	5759
2:2:3	39.49	20.47	40.04	1.889	− 28.13	8.94	37.13	5874
2:3:1	47.28	36.75	15.97	1.856	− 35.83	8.62	34.14	5614
2:3:2	40.76	31.69	27.55	1.861	− 33.88	8.69	34.79	5693
2:3:3	35.83	27.85	36.32	1.865	− 32.39	8.75	35.29	5753
3:1:1	71.53	12.36	16.11	1.956	− 20.47	9.34	41.29	6018
3:1:2	61.60	10.65	27.75	1.947	− 20.63	9.31	40.98	6042
3:1:3	54.09	9.35	36.56	1.940	− 20.75	9.29	40.74	6060
3:2:1	63.66	22.00	14.34	1.917	− 26.36	9.06	38.42	5859
3:2:2	55.68	19.24	25.08	1.914	− 25.76	9.07	38.51	5901
3:2:3	49.47	17.09	33.44	1.912	− 25.30	9.08	38.57	5933
3:3:1	57.35	29.73	12.92	1.887	− 31.08	8.84	36.26	5731
3:3:2	50.79	26.33	22.88	1.888	− 30.00	8.87	36.58	5784

had outstanding energetic performance and superior power. Besides, these data also indicate that CL-20 was a kind of splendid and promising HEDMs. For CL-20/TNT, CL-20/HMX, or CL-20/TNT/HMX cocrystal explosives, the density declined and detonation parameters were also decreased, namely, the power and energetic performance was weakened. The CL-20/TNT/HMX cocrystal model with the molar ratio of 1:3:1 had the least value of density and detonation parameters and it was 1.806 g/cm^3, 8.27 km/s, 30.98 GPa, and 5423 kJ/kg, respectively. This further implied that the cocrystal model also exhibited the poorest detonation performance and lowest energy density. On the contrary, the cocrystal model with a molar ratio of 3:1:1 had the highest density and maximal detonation velocity and detonation pressure, corresponding to 1.956 g/cm^3, 9.34 km/s, 41.29 GPa, and 6018 kJ/kg. Previous studies [50–52] have clearly stated that for HEDMs, it was required that $\rho > 1.9$ g/cm^3, $D >$ 9.2 km/s, $P > 40$ GPa. Among the whole CL-20/TNT/HMX cocrystal models, only the cocrystal model with the molar ratio of 3:1:1, 3:1:2, 3:1:3 could satisfy the requirement.

Mechanical properties

Mechanical properties were generally characterized by five parameters, i.e., tensile modulus (*E*), shear modulus (*G*), bulk modulus (*K*), Poisson's ratio (ν), and Cauchy pressure (C_{12}-C_{44}). Among them, *E*, *K*, and *G* were also called the engineering modulus. *E*, *K*, and *G* was commonly applied as a criterion to evaluate the rigidity, stiffness, or hardness of a material. Besides, *K* was an important level to reflect the rupture strength and materials with higher value of *K* would also have greater rupture strength [53]. Cauchy pressure was commonly

Table 10 Mechanical properties of raw components, CL-20/TNT, CL-20/HMX, and CL-20/TNT/HMX cocrystal models[a]

Substituted pattern	Mechanical properties	1:0:0	0:1:0	0:0:1	1:1:0	2:0:1	1:1:1	1:1:2	1:1:3	1:2:1	1:2:2
(1 0 0)	E	17.735	9.675	12.615	13.083	14.500	13.907	14.573	14.173	11.891	12.572
	ν	0.229	0.228	0.229	0.226	0.227	0.226	0.227	0.229	0.226	0.227
	K	10.903	5.932	7.766	7.968	8.865	8.471	8.913	8.725	7.237	7.689
	G	7.216	3.939	5.131	5.334	5.907	5.670	5.936	5.765	4.849	5.121
	C_{12}-C_{44}	− 3.812	− 0.384	− 1.771	1.349	− 0.216	− 0.202	− 0.514	− 0.036	0.636	0.358
(0 1 0)	E	15.025	7.746	10.981	10.091	11.996	12.446	11.972	12.388	10.648	11.363
	ν	0.230	0.227	0.224	0.229	0.231	0.228	0.225	0.227	0.231	0.227
	K	9.267	4.726	6.623	6.203	7.423	7.636	7.252	7.558	6.589	6.932
	G	6.109	3.157	4.487	4.106	4.874	5.066	4.887	5.049	4.326	4.631
	C_{12}-C_{44}	− 2.565	0.209	− 1.295	2.319	0.151	0.621	0.257	0.339	0.803	0.517
(0 0 1)	E	16.165	9.441	12.180	11.944	13.141	13.692	13.904	14.185	12.702	12.030
	ν	0.229	0.225	0.228	0.229	0.232	0.227	0.228	0.226	0.225	0.229
	K	9.932	5.725	7.453	7.362	8.158	8.369	8.507	8.642	7.703	7.415
	G	6.578	3.853	4.961	4.857	5.335	5.578	5.663	5.783	5.184	4.892
	C_{12}-C_{44}	− 3.187	− 0.401	− 1.525	1.782	− 0.468	0.177	− 0.183	− 0.372	0.275	0.713
Random	E	15.585	8.584	11.613	10.858	12.482	12.640	12.603	12.278	11.497	12.121
	ν	0.226	0.228	0.230	0.229	0.227	0.231	0.228	0.226	0.229	0.227
	K	9.475	5.266	7.182	6.673	7.609	7.819	7.732	7.464	7.065	7.389
	G	6.357	3.494	4.719	4.418	5.088	5.136	5.130	5.008	4.678	4.941
	C_{12}-C_{44}	− 2.934	− 0.105	− 1.824	1.816	− 0.375	0.305	− 0.415	− 0.207	0.355	0.571
Substituted pattern	Mechanical properties	1:2:3	1:3:1	1:3:2	1:3:3	2:1:1	2:1:2	2:1:3	2:2:1	2:2:3	2:3:1
(1 0 0)	E	12.802	12.568	12.339	11.254	14.268	13.890	13.752	13.591	13.102	13.029
	ν	0.230	0.227	0.226	0.229	0.227	0.230	0.226	0.229	0.230	0.227
	K	7.917	7.661	7.501	6.917	8.697	8.590	8.361	8.353	8.103	7.942
	G	5.202	5.123	5.033	4.579	5.816	5.644	5.609	5.530	5.324	5.311
	C_{12}-C_{44}	0.239	0.620	0.534	0.782	0.174	0.325	0.218	0.836	0.778	0.236
(0 1 0)	E	11.047	11.209	10.463	11.476	12.421	11.575	11.361	11.083	11.767	11.937
	ν	0.226	0.227	0.228	0.227	0.225	0.229	0.227	0.231	0.228	0.229
	K	6.716	6.834	6.419	6.996	7.532	7.114	6.926	6.856	7.219	7.336
	G	4.506	4.569	4.259	4.678	5.069	4.710	4.631	4.503	4.790	4.857
	C_{12}-C_{44}	0.368	0.815	0.497	0.642	0.683	0.725	0.487	1.136	0.749	0.718
(0 0 1)	E	12.254	11.796	11.345	12.083	13.048	13.972	13.424	12.998	12.674	12.669
	ν	0.228	0.230	0.230	0.225	0.228	0.225	0.227	0.226	0.228	0.230
	K	7.518	7.295	7.016	7.327	8.005	8.472	8.183	7.902	7.776	7.835
	G	4.988	4.793	4.610	4.931	5.311	5.702	5.472	5.302	5.159	5.148
	C_{12}-C_{44}	0.369	0.873	0.826	0.571	0.387	0.234	0.438	1.105	0.923	0.749
Random	E	12.146	11.305	10.831	11.603	12.408	12.911	12.722	12.050	12.349	12.554
	ν	0.227	0.226	0.229	0.228	0.230	0.225	0.225	0.227	0.227	0.228
	K	7.404	6.872	6.657	7.118	7.653	7.829	7.714	7.346	7.528	7.702
	G	4.951	4.611	4.407	4.723	5.045	5.269	5.192	4.912	5.034	5.110
	C_{12}-C_{44}	0.484	1.006	1.105	0.502	0.919	1.004	1.257	0.631	0.585	0.816
Substituted pattern	Mechanical properties	2:3:2	2:3:3	3:1:1	3:1:2	3:1:3	3:2:1	3:2:2	3:2:3	3:3:1	3:3:2
(1 0 0)	E	13.834	14.047	12.485	10.382	11.294	13.506	11.976	13.021	12.676	13.266
	ν	0.229	0.228	0.230	0.234	0.230	0.226	0.228	0.226	0.227	0.229
	K	8.502	8.618	7.721	6.517	6.985	8.211	7.348	7.916	7.728	8.154
	G	5.629	5.718	5.073	4.205	4.589	5.509	4.875	5.311	5.167	5.398
	C_{12}-C_{44}	0.115	0.304	1.026	1.557	1.383	0.334	0.537	0.702	1.465	0.934
(0 1 0)	E	12.190	11.561	10.605	10.718	9.901	12.308	11.876	11.435	11.970	11.741
	ν	0.227	0.228	0.229	0.227	0.234	0.231	0.228	0.227	0.230	0.227

Table 10 (continued)

	K	7.431	7.092	6.517	6.534	6.215	7.614	7.286	6.971	7.402	7.157
	G	4.969	4.706	4.315	4.369	4.010	5.001	4.834	4.661	4.864	4.786
	C_{12}-C_{44}	1.101	0.626	1.382	1.114	1.469	0.835	0.914	0.619	0.926	0.699
(0 0 1)	E	13.438	12.943	10.804	10.404	10.602	12.955	12.089	12.311	12.050	13.394
	ν	0.226	0.230	0.228	0.227	0.231	0.226	0.228	0.228	0.229	0.229
	K	8.170	8.005	6.628	6.343	6.571	7.875	7.417	7.553	7.406	8.232
	G	5.481	5.259	4.398	4.241	4.306	5.284	4.921	5.011	4.903	5.450
	C_{12}-C_{44}	0.502	0.617	1.283	1.646	1.115	0.787	0.526	0.530	0.671	0.545
Random	E	12.415	12.469	10.200	10.789	11.067	12.396	11.629	12.109	12.219	12.883
	ν	0.227	0.230	0.228	0.228	0.229	0.227	0.231	0.226	0.228	0.229
	K	7.568	7.711	6.258	6.619	6.801	7.557	7.193	7.362	7.225	7.917
	G	5.061	5.067	4.152	4.392	4.503	5.053	4.725	4.939	4.794	5.242
	C_{12}-C_{44}	0.823	0.937	1.511	0.924	0.708	0.802	0.553	0.471	0.904	0.726

[a] Units for E, K, G, and (C_{12}-C_{44}) are in GPa, ν has no units

used to estimate the ductility, plastic property, or brittle property of a material [54]. In other words, a high positive value of (C_{12}-C_{44}) would mean that the material had desirable ductility or superior plastic property. On the contrary, if the value of (C_{12}-C_{44}) was negative, it would indicate that the material exhibited a brittle property.

Mechanical properties were generally depicted by elastic coefficients (C_{ij}), stress (σ), and strain (ε) as follows [55, 56]:

$$\sigma_i = C_{ij}\varepsilon_j \tag{9}$$

Bulk modulus (K) and shear modulus (G) were illustrated as follows:

$$K_R = [S_{11} + S_{22} + S_{33} + 2(S_{12} + S_{23} + S_{31})]^{-1} \tag{10}$$

$$G_R = 15[4(S_{11} + S_{22} + S_{33}) - 4(S_{12} + S_{23} + S_{31}) + 3(S_{44} + S_{55} + S_{66})]^{-1} \tag{11}$$

where the subscript R is the Reuss average and the parameters (S_{ij}) and elastic coefficients (C_{ij}) are illustrated as $\boldsymbol{S}=\boldsymbol{C}^{-1}$.

Mechanical properties could be related together as follows:

$$E = 2G(1 + \nu) = 3K(1-2\nu) \tag{12}$$

Based on the above equations, tensile modulus (E) and Poisson's ratio (ν) could be calculated as that:

$$E = \frac{9GK}{3K + G} \tag{13}$$

$$\nu = \frac{3K-2G}{2(3K + G)} \tag{14}$$

The mechanical properties of CL-20, TNT, HMX, CL-20/TNT, CL-20/HMX, and CL-20/TNT/HMX cocrystal explosives are listed in Table 10.

What can be concluded from Table 10 is that both the raw components (CL-20, TNT, and HMX), CL-20/TNT, CL-20/HMX, and CL-20/TNT/HMX cocrystal explosives had different mechanical properties. Among the whole crystal models, CL-20 had the highest value of E, K, G, but the lowest Cauchy pressure (C_{12}-C_{44}). In other words, the value of E, K, G for pure CL-20 was very high, while Cauchy pressure (C_{12}-C_{44}) was negative. For example, the value of E, K, G for (0 0 1) crystal surface was 16.165, 9.932, and 6.578 GPa, respectively. The high and positive value of E, K, G might mean that the stiffness, rigidity, hardness, or rupture strength of CL-20 was very good. However, the negative value of Cauchy pressure (− 3.187 GPa) indicates that CL-20 presented poor ductility and plastic property. Consequently, the mechanical properties or raw CL-20 was undesirable. For CL-20/TNT, CL-20/HMX, and CL-20/TNT/HMX cocrystal models, the three engineering moduli (E, K, G) were decreased, while Cauchy pressure was increased, thus implying that the rigidity and hardness of cocrystal models was lower than CL-20, but the plastic property was better than CL-20, namely, the cocrystal model had better mechanical properties than CL-20. Besides, the variation of mechanical properties also illustrated that cocrystallization could effectively improve mechanical properties of ECs. Table 10 also illustrates that the value of E, K, G of different substituted patterns varied as (1 0 0) > (0 0 1) > random > (0 1 0), while Cauchy pressure was on the opposite order. Therefore, (1 0 0) crystal surface exhibited the highest rigidity, but poorest ductility, while (0 1 0) surface held the most desirable mechanical properties. What's more, for (1 0 0) and (0 0 1) crystal surfaces, when the molar ratio was 3:1:2, the CL-20/TNT/HMX cocrystal model held the lowest E, K, G, but the largest Cauchy pressure, i.e., this cocrystal model had the best mechanical properties. For (0 1 0) crystal surface, the cocrystal model presented the best mechanical properties with a molar ratio of 3:1:3 and it was 3:1:1 for a random substituted pattern.

When taking the stability, sensitivity, energetic performance, and mechanical properties into consideration, it could be concluded that when the molar ratio of different components was 3:1:1, 3:1:2, or 3:1:3, the CL-20/TNT/HMX cocrystal explosive had the most desirable or superior properties and might be formed more probably, especially the cocrystal model with molar ratio of 3:1:2. Consequently, the cocrystal explosives with these molar ratios were very promising and worth more attention.

Conclusions

In this work, the pure CL-20, TNT, HMX, CL-20/TNT, CL-20/HMX, and CL-20/TNT/HMX cocrystal explosive models were established and MD method was applied to predict the stability, sensitivity, energetic performance, and mechanical properties of different crystal models. The influences of co-crystallization and molar ratios on properties of cocrystal explosives were investigated and estimated. The main results and conclusions are listed as follows:

(1) The CL-20/TNT/HMX cocrystal explosive with molar ratio of 3:1:2 or 3:1:3 had the largest binding energy and best stability. The cocrystal model might be more likely to be formed with these molar ratios. (0 1 0) crystal surface was more stable than (0 0 1), (1 0 0) and random substituted models.
(2) The cocrystal model had less value of trigger bond length, but higher value of trigger bond energy and CED than CL-20, i.e., cocrystal model had lower mechanical sensitivity and better safety. The CL-20/TNT/HMX cocrystal model with a molar ratio of 3:1:2 was the most insensitive cocrystal model and exhibited the best safety.
(3) The detonation parameters and energetic performance of CL-20/TNT/HMX cocrystal explosive was lower than pure CL-20, only the cocrystal model with molar ratio of 3:1:1, 3:1:2, or 3:1:3 exhibited desirable detonation performance and could satisfy the requirement of HEDMs.
(4) The cocrystal explosive presented better mechanical properties than CL-20 and the CL-20/TNT/HMX cocrystal explosive with molar ratios of 3:1:1, 3:1:2, or 3:1:3 had the most desirable mechanical properties.

In a word, co-crystallization could effectively decrease mechanical sensitivity, strengthen safety, improve mechanical properties, and transform energetic performance. The CL-20/TNT/HMX cocrystal explosive with molar ratio of 3:1:2 exhibited the best stability, lowest mechanical sensitivity, and excellent safety. Besides, this cocrystal model also had superior energetic performance and desirable mechanical properties. Therefore, this CL-20/TNT/HMX cocrystal model had the best comprehensive properties and was very promising. This work could provide some theoretical support and helpful guidance to better clarify the cocrystal mechanism and design new kinds of energetic cocrystals.

References

1. Agrawal JP (1998) Recent trends in high-energy materials. Prog Energy Combust Sci 24:1–30
2. Sikder AK, Sikder N (2004) A review of advanced high performance, insensitive and thermally stable energetic materials emerging for military and space applications. J Hazard Mater 112:1–15
3. Lara OF, Espinosa PG (2007) Cocrystals definitions. Supramol Chem 19:553–557
4. Shan N, Zaworotko MJ (2008) The role of cocrystals in pharmaceutical science. Drug Discov Today 13:440–446
5. Guo CY, Zhang HB, Wang XC, Xu JJ, Liu Y, Liu XF, Huang H, Sun J (2013) Crystal structure and explosive performance of a new CL-20/caprolactam cocrystal. J Mol Struct 1048:267–273
6. Xu HF, Duan XH, Li HZ, Pei CH (2015) A novel high-energetic and good-sensitive cocrystal composed of CL-20 and TATB by a rapid solvent/non-solvent method. RSC Adv 5:95764–95770
7. Yang ZW, Li HZ, Zhou XQ, Zhang CY, Huang H, Li JS, Nie FD (2012) Characterization and properties of a novel energetic–energetic cocrystal explosive composed of HNIW and BTF. Cryst Growth Des 12:5155–5158
8. Wu JT, Zhang JG, Li T, Li ZM, Zhang TL (2015) A novel cocrystal explosive NTO/TZTN with good comprehensive properties. RSC Adv 5:28354–28359
9. Landenberger KB, Bolton O, Matzger AJ (2013) Two isostructural explosive cocrystals with significantly different thermodynamic stabilities. Angew Chem Int Ed 52:6468–6471
10. Lin H, Chen JF, Zhu SG, Li HZ, Huang Y (2017) Synthesis, characterization, detonation performance, and DFT calculation of HMX/PNO cocrystal explosive. J Energ Mater 35:95–108
11. Zhang HB, Guo CY, Wang XC, Xu JJ, He X, Liu Y, Liu XF, Huang H, Sun J (2013) Five energetic cocrystals of BTF by intermolecular hydrogen bond and π-stacking interactions. Cryst Growth Des 13:679–687
12. Bolton O, Simke LR, Pagoria PF, Matzger AJ (2012) High-power explosive with good sensitivity: a 2:1 cocrystal of CL-20:HMX. Cryst Growth Des 12:4311–4314
13. Yang ZW, Li HZ, Huang H, Zhou XQ, Li JS, Nie FD (2013) Preparation and performance of a HNIW/TNT cocrystal explosive. Propellants Explos Pyrotech 38:495–501
14. Agrawal JP (2005) Some new high-energy materials and their formulations for specialized applications. Propellants Explos Pyrotech 30:316–328
15. Foltz MF, Coon CL, Garcia F, Nichols AL (1994) The thermal stability of the polymorphs of hexanitrohexaazaisowurtzitane, part I. Propellants Explos Pyrotech 19:19–25
16. Chang SC, Henry PB (1970) A study of the crystal structure of β-cyclotetramethylene tetranitramine by neutron diffraction. Acta Crystallogr B 26:1235–1240
17. Cady HH, Larson AC, Cromer DT (1963) The crystal of α-HMX and a refinement of the structure of β-HMX. Acta Crystallogr 16:617–623

18. Zhao XQ, Shi NC (1995) Crystal structure of ε-hexanitrohexaazaisowurtzitane. Chin Sci Bull 40:2158–2160
19. Vrcelj RM, Sherwood JN, Kennedy AR, Gallagher HG, Gelbrich T (2003) Polymorphism in 2-4-6 trinitrotoluene. Cryst Growth Des 3: 1027–1032
20. Liu K, Zhang G, Luan JY, Chen ZQ, Su PF, Shu YJ (2016) Crystal structure, spectrum character and explosive property of a new cocrystal CL-20/DNT. J Mol Struct 110:91–96
21. Lin H, Zhu SG, Li HZ, Peng XH (2013) Structure and detonation performance of a novel HMX/LLM-105 cocrystal explosive. J Phys Org Chem 26:898–907
22. Wang YP, Yang ZW, Li HZ, Zhou XQ, Zhang Q, Wang JH, Liu YC (2014) A novel cocrystal explosive of HNIW with good comprehensive properties. Propellants Explos Pyrotech 39:590–596
23. Lin H, Zhu SG, Zhang L, Peng XH, Chen PY, Li HZ (2013) Intermolecular interactions, thermodynamic properties, crystal structure, and detonation performance of HMX/NTO cocrystal explosive. Int J Quantum Chem 113:1591–1599
24. Guo CY, Zhang HB, Wang XC, Liu XF, Sun J (2013) Study on a novel energetic cocrystal of TNT/TNB. J Mater Sci 48:1351–1357
25. Landenberger KB, Matzger AJ (2010) Cocrystal engineering of prototype energetic material: supramolecular chemistry of 2,4,6-trinitrotoluene. Cryst Growth Des 10:5341–5347
26. Sun H, Ren PJ, Fried R (1998) The COMPASS force field: parameterization and validation for phosphazenes. Comput Theor Polym Sci 8:229–246
27. Bunte SW, Sun H (2000) Molecular modeling of energetic materials: the parameterization and validation of nitrate esters in the COMPASS forcefield. J Chem Chem B 104:2477–2489
28. Michael JM, Sun H, Rigby D (2004) Development and validation of COMPASS force field parameters for molecules with aliphatic azide chains. J Comput Chem 25:61–71
29. Xu XJ, Xiao HM, Xiao JJ, Zhu W, Huang H, Li JS (2006) Molecular dynamics simulations for pure ε-CL-20 and ε-CL-20-based PBXs. J Phys Chem B 110:7203–7207
30. Qiu L, Xiao HM (2009) Molecular dynamics study of binding energies, mechanical properties, and detonation performances of bicyclo-HMX-based PBXs. J Hazard Mater 164:329–336
31. Ma XF, Xiao JJ, Huang H, Ju XH, Li JS, Xiao HM (2006) Simulative calculation of mechanical property, binding energy and detonation property of TATB/fluorine-polymer PBX. Chin J Chem 24:473–477
32. Zhu W, Xiao JJ, Zhu WH, Xiao HM (2009) Molecular dynamics simulations of RDX and RDX-based plastic-bonded explosives. J Hazard Mater 164:1082–1088
33. Xiao JJ, Wang WR, Chen J, Ji GF, Zhu W, Xiao HM (2012) Study on the relations of sensitivity with energy properties for HMX and HMX-based PBXs by molecular dynamics simulation. Physica B 407:3504–3509
34. Politzer P, Murray JS (2015) Impact sensitivity and maximum heat of detonation. J Mol Model 21:262
35. Politzer P, Murray JS, Clark T (2015) Mathematical modeling and physical reality in noncovalent interactions. J Mol Model 21:52
36. Stephen AD, Kumarashas P, Pawar RB (2011) Charge density distribution, electrostatic properties, and impact sensitivity of the high energetic molecule TNB: a theoretical charge density study. Propellants Explos Pyrotech 36:168–174
37. Politzer P, Murray JS (2016) High performance, low sensitivity: conflicting or compatible. Propellants Explos Pyrotech 41:414–425
38. Zhu W, Wang XJ, Xiao JJ, Zhu WH, Sun H, Xiao HM (2009) Molecular dynamics simulations of AP/HMX composite with a modified force field. J Hazard Mater 167:810–816
39. Xiao JJ, Li SY, Chen J, Ji GF, Zhu W, Zhao F, Wu Q, Xiao HM (2013) Molecular dynamics study on the correlation between structure and sensitivity for defective RDX crystals and their PBXs. J Mol Model 19:803–809
40. Sun T, Xiao JJ, Liu Q, Zhao F, Xiao HM (2014) Comparative study on structure, energetic and mechanical properties of a ε-CL-20/HMX cocrystal and its composite with molecular dynamics simulation. J Mater Chem A 2:13898–13904
41. Xiao JJ, Zhao L, Zhu W, Chen J, Ji GF, Zhao F, Wu Q, Xiao HM (2012) Molecular dynamics study on the relationships of modeling, structural and energy properties with sensitivity for RDX-based PBXs. Sci China Chem 55:2587–2594
42. Xiao JJ, Wang WR, Chen J, Ji GF, Zhu W, Xiao HM (2012) Study on structure, sensitivity and mechanical properties of HMX and HMX-based PBXs with molecular dynamics simulation. Comput Theor Chem 999:21–27
43. Xu XJ, Xiao HM, Ju XH, Gong XD (2005) Theoretical study on pyrolysis mechanism for ε-hexanitrohexaazaisowurtzitane. Chin J Org Chem 25:536–539
44. Geetha M, Nair UR, Sarwade DB, Gore GM, Asthana SN, Singh H (2003) Studies on CL-20: the most powerful high energy material. J Therm Anal Calorim 73:913–922
45. Guo YX, Zhang HS (1983) Nitrogen equivalent coefficient and revised nitrogen equivalent coefficient equations for calculating detonation properties of explosives: detonation velocity of explosives. Explos Shock Waves 3:57–65
46. Wang YL, Yu WL (2011) Explosives, initiators and pyrotechnics. Northwestern Polytechnical University Press, Xi'an
47. Hang GY, Yu WL, Wang T, Wang JT, Li Z (2017) Comparative studies on structures, mechanical properties, sensitivity, stabilities and detonation performance of CL-20/TNT cocrystal and composite explosives by molecular dynamics simulation. J Mol Model 23:281
48. Ou YX (2006) Explosives. Beijing Institute of Technology Press, Beijing
49. Jin SH, Song QC (2010) Explosive theory. Northwestern Polytechnical University Press, Xi'an
50. Xiao HM, Xu XJ, Qiu L (2008) Theoretical design of high energy density materials. Science Press, Beijing
51. Xu XJ, Xiao JJ, Huang H, Li JS, Xiao HM (2007) Molecular dynamics simulations on the structures and properties of ε-CL-20-based PBXs-primary theoretical studies on HEDM formulation design. Sci China Ser B Chem 50:737–745
52. Xu XJ, Xiao HM, Ju XH, Gong XD, Zhu WH (2006) Computational studies on polynitrohexaazaadmantanes as potential high energy density materials (HEDMs). J Phys Chem A 110: 5929–5933
53. Pugh SF (1954) Relations between the elastic moduli and the plastic properties of polycrystalline pure metals. Philos Mag 45:823–843
54. Pettifor DG (1992) Theoretical predictions of structure and related properties of intermetallics. Mater Sci Technol 8:345–349
55. Wu JL (1993) Mechanics of elasticity. Tongji University Press, Shanghai
56. Weiner JH (1983) Statistical mechanics of elasticity. Wiley, New York